The Asymptotes of Loop Reactors

Moshe Sheintuch and Olga Nekhamkina
Dept. of Chemical Engineering, Technion–Israel Institute of Technology (IIT), Technion City, Haifa 32 000, Israel

DOI 10.1002/aic.10287
Published online in Wiley InterScience (www.interscience.wiley.com).

Loop reactors extend the flow-reversal concept to rotating port feeding in a loop-shape system made of N units. To analyze its behavior two limiting models are derived for a system with an infinite number of units: The first one corresponds to an arbitrary switching velocity, whereas the second corresponds to large switching velocities and is essentially a cross-flow model. Both models can admit, with a generic first-order Arrhenius kinetics and typically large Pe and Le numbers, a rotating-pulse solution with peak temperatures that significantly exceeds the increase in adiabatic temperature. Both solutions were corroborated by simulations of finite-N systems that show convergence to the expected asymptotes in realistic system lengths. Rotating pulses emerge over a wide domain of parameters, when the ratio of switching velocity to front propagation velocity is properly tuned around unity, and in a relatively narrow domain of parameters, around the Hopf bifurcation to spatial oscillations, when that ratio is high. Between these two (slow- and fast-switching) behaviors the system exhibits a complex structure of solutions. The asymptotic models enabled us to draw bifurcation diagrams and characterize the properties of emerging solutions. Future studies will apply the loop reactor concept to reversible reactions and endothermic–exothermic reactions. © 2004 American Institute of Chemical Engineers *AIChE J,* 51: 224–234, 2005

Introduction

The design of a catalytic reactor with a single reaction may be aimed to achieve the highest temperature, which usually implies the highest conversion, or to achieve as homogeneous (uniform) working conditions as possible, or to achieve a certain optimal profile. Flow-reversal reactors, in which the reactants are fed at two ports, rather than the one-port feed of traditional catalytic reactors, are currently attracting intensive research and have been applied commercially. The advantage of reactors with periodic flow reversal over simple once-through operation for attaining high temperatures has been demonstrated in many studies of adiabatic units during the past decade. This feature results from the nature of heat loss in the two reactors: In a simple adiabatic fixed bed the reaction heat is dissipated by convection, whereas in the flow-reversal unit, with fast switching, heat is lost mainly by conduction, and this term can be mitigated by building long inert zones on both sides of the catalytic layer. This feature makes flow-reversal units especially attractive for catalytic volatile organic compound (VOC) oxidation or NO reduction, if the temperature of the hot zone can exceed the ignition point of the dilute-reactant stream[1-3] (for a recent review, see Kolios et al.[4]). The main advantage of a reactor with flow reversal for combustion purposes is that the bed temperature increases with the flow rate into the reactor, as more material is consumed. Other applications of this technology were aimed at improving conversion of exothermic reversible equilibrium-limited reactions such as SO_2 oxidation[5,6] and methanol or ammonia synthesis.[7-9]

Loop reactors extend the two-port concept into feeding at several or many ports in several reactor units that are organized in a loop. To illustrate this concept consider a loop reactor with N units (1, 2, . . . , N), with a feed port and an exit port that are switched at every predetermined time interval σ. We can consider the following approaches:

(1) In the compact loop reactor all N units are used at all times: In the first interval we feed through unit 1, whereas the flow exits at the end of unit N; in the second interval the flow

Correspondence concerning this article should be addressed to M. Sheintuch at cermsll@tx.technion.ac.il.

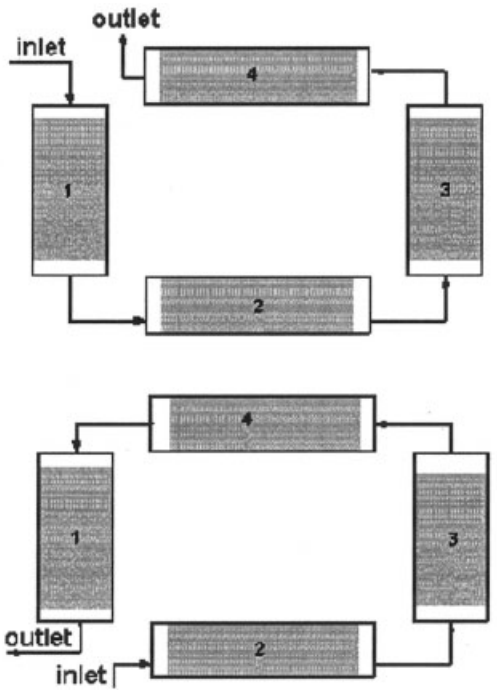

Figure 1. Two consecutive feed positions (out of four) in a loop reactor with a compact scheme.

enters at unit 2 and exits from section 1, and so on (see Figure 1 for two steps in a four-reactor system). Thus, the feed and exit streams are adjacent, which requires special arrangement and control of valves. This approach was studied numerically by Barresi's group.[10-14]

(2) In the *noncompact approach*, in the first interval we feed through unit 1, whereas the flow exits from unit $N-1$; in the second interval the flow enters at unit 2 and exits unit N, and so on. This approach makes less-efficient use of the catalyst but requires fewer valves and tubes.

The advantage of loop reactors is that better performance may be achieved in a processing unit with no boundaries and with feed dispersion along the reactor; this idea has been implemented in chromatographic separation. Heat loss by conduction in a loop reactor depends on its structure: in a true loop design there are no edges and dissipation by conduction can be eliminated, and we may find higher temperatures than those in flow reversal. Also, in loop reactors with rotating hot-spot patterns, the deactivation is less severe than that in the other two reactors because it is averaged over the whole reactor. This design, however, requires complexity in terms of lines, valves, and control. Several numerical solutions of loop reactors have been published by Barresi's group for certain applications such as abatement of VOCs[10,11] and exothermic reversible gas synthesis reactions.[12-14]

Here, we seek to generalize these results by studying the asymptotic solutions of loop reactors, in which a single exothermic reaction occurs. To understand the approximations to the problem let us review the timescales associated with it. The residence time in the reactor is typically 1 s or a fraction of it, whereas the front velocity is typically of $O(0.001$ m/s). A noticeable front displacement will thus take 1000 s or so. Between these two timescales, we can switch port every 10–200 s. After switching it will take a few seconds (that is, several residence times) for the mass balance to readjust itself, whereas the temperature profile can be assumed to be constant for that duration. The difference of the timescales is an essential prerequisite for emergence of various patterns that can be controlled in a loop reactor by appropriate choice of the switching intervals (external forcing). Specifically, we show that rotating patterns may emerge in such reactors, provided that the switching velocity (that is, unit length/switching time) and the pattern velocity are matched in a certain way. More precisely we will explain below two such asymptotes in which the ratio of the two velocities is either around unity, which we will refer to as *slow switching*, or very large, which we will refer to as *fast switching*. The former will be shown to yield performance somewhat similar to that of a flow reversal reactor, whereas the latter corresponds to a cross-flow reactor.[15-17] Between these two asymptotes, the dynamics may become very complex, in a way that can be described as a rotating pulse forced externally and is reminiscent of the forced-oscillator problem.

Loop reactors at both asymptotes can attain patterns that exhibit a high-temperature hot spot that may compete with those of other approaches, such as the flow-reversal reactors. This approach should be contrasted, therefore, with the flow-reversal reactor and, specifically, we seek to determine whether a loop reactor with a small number of ports (say four) will achieve a solution that is superior to warrant the complexity required for the construction. We limit our study to generic first-order activated and exothermic processes.

The structure of this work is the following: in the next section we formulate the multiunit reactor model and derive its two asymptotes corresponding to: (1) a system with an infinite number of ports, and (2) an infinite-port model in the case of fast switching. In the third section we analyze the limiting continuous models and the corresponding pattern-formation mechanisms in the case of slow switching. The fast-switching case is studied in section four, whereas intermediate switching is considered in section five. For all types of switching the analytical predictions are compared with results of numerical simulations of a finite-unit reactor model with various numbers of sections and convergence to the asymptotic models is demonstrated. In conclusion we comment on future extension of the proposed limiting models.

Reactor Models

Consider a pseudo-homogeneous one-dimensional (1-D) model of an adiabatic catalytic bed reactor in which a reaction of a general kinetics occurs [$r(T, C)$ is the rate]. The enthalpy and mass balances are described by

$$(\rho c_p)_e \frac{\partial T}{\partial t} + (\rho c_p)_f u \frac{\partial T}{\partial z} - k_e \frac{\partial^2 T}{\partial z^2} = (-\Delta H)(1-\varepsilon)\rho r(C, T)$$
$$\frac{\partial C}{\partial t} + u \frac{\partial C}{\partial z} - \varepsilon D_f \frac{\partial^2 C}{\partial z^2} = (1-\varepsilon)\rho r(C, T) \qquad (1)$$

with appropriate initial $C(0, z) = C^0(z)$, $T(0, z) = T^0(z)$ and boundary conditions (BC; typically Danckwerts' type with $z_{in} = 0$, $z_{out} = \tilde{L}$)

$$z = z_{in} \qquad \varepsilon D_f \frac{\partial C}{\partial z} = u(C - C^{in}) \qquad k_e \frac{\partial T}{\partial z} = (\rho C_p)_f u(T - T^{in})$$
$$z = z_{out} \qquad \frac{\partial T}{\partial z} = \frac{\partial C}{\partial z} = 0 \tag{2}$$

We limit our study to generic first-order activated and exothermic reactions with a rate of $r = A \exp(-E/RT)C$. To a first approximation the transport coefficients (k_e, D_f) and thermodynamic parameters (ρ, c_p) are assumed to be fixed. With these assumptions the system of Eqs. 1 and 2 may be rewritten in the dimensionless form as

$$\mathrm{Le}\frac{\partial y}{\partial \tau} + \nu \frac{\partial y}{\partial \xi} - \frac{1}{\mathrm{Pe}_y}\frac{\partial^2 y}{\partial \xi^2} = B\,\mathrm{Da}(1-x)\exp\left(\frac{\gamma y}{\gamma + y}\right)$$
$$\frac{\partial x}{\partial \tau} + \nu \frac{\partial x}{\partial \xi} - \frac{1}{\mathrm{Pe}_x}\frac{\partial^2 x}{\partial \xi^2} = \mathrm{Da}(1-x)\exp\left(\frac{\gamma y}{\gamma + y}\right) \tag{3}$$

$$\tau = 0 : y(0, z) = y^0 \qquad x(0, z) = -x^0$$
$$\xi = \xi_{in} \qquad \frac{1}{\mathrm{Pe}_y}\frac{\partial y}{\partial \xi} = \nu(y - y^{in}) \qquad \frac{1}{\mathrm{Pe}_x}\frac{\partial x}{\partial \xi} = \nu(x - x^{in})$$
$$\xi = \xi_{out} \qquad \frac{\partial y}{\partial \xi} = 0 \qquad \frac{\partial x}{\partial \xi} = 0 \tag{4}$$

Here the conventional notation is used

$$x = 1 - \frac{C}{C_0} \qquad y = \gamma \frac{T - T_0}{T_0} \qquad \xi = \frac{z}{z_0}$$
$$\tau = \frac{t u_0}{z_0} \qquad \nu = \frac{u}{u_0} \qquad L = \frac{\tilde{L}}{z_0}$$
$$\gamma = \frac{E}{RT_{in}} \qquad B = \gamma \frac{(-\Delta H)C_0}{(\rho c_p)_f T_0}$$
$$\mathrm{Da} = \frac{L(1-\varepsilon)A}{u_0}\, e^{-\gamma} \qquad \mathrm{Le} = \frac{(\rho c_p)_e}{(\rho c_p)_f}$$
$$\mathrm{Pe}_y = \frac{(\rho c_p)_f z_0 u_0}{k_e} \qquad \mathrm{Pe}_x = \frac{z_0 u_0}{\varepsilon D_f}$$

Note, that we use arbitrary values u_0, z_0 for the velocity and the length scales to ensure that the corresponding dimensionless values (L, v) can be varied as independent parameters. Typically in our simulations, as well as in practical situations, $\mathrm{Le} \gg 1$ and Pe_x, $\mathrm{Pe}_y \gg 1$.

Multiport reactor

Consider a loop reactor of N identical units (each one of the length $\Delta L = L/N$), with gradual switching of the inlet/outlet ports over each time interval σ. Such a reactor can be described by a continuous model (Eqs. 3 and 4) if we ignore the edge effects of the intermediate sections and apply the boundary conditions at positions that vary in time as stepwise functions with a total period $\theta = N\sigma$

$$\xi_{in} = (n-1)\Delta L \qquad t \in [(n-1)\sigma, n\sigma] + k\theta$$
$$n = 1, \ldots, N \qquad k = 0, 1, \ldots \tag{5}$$

Here n specifies the unit number and k is the cycle number. The outlet position almost coincides with the inlet in the compact organization scheme (in this case it is useful to define the boundaries as $\xi_{in} = \xi_b^+$, $\xi_{out} = \xi_b^-$), whereas in the noncompact organization ξ_{out} follows ξ_{in} (Eq. 5) with a prescribed length of the active reactor between them.

Simulations of fast switching (see below) have shown that in many cases feed switching induces a local extinction at that point, attributed to the cold feed, and the front eventually propagates and leads to the reactor extinction. With a heterogeneous model we expect this effect to be less severe because the decline of the fluid temperature will not immediately affect the solid temperature because of the large heat capacity. A similar effect can be achieved with a pseudo-homogeneous model that accounts for a narrow inert entrance zone of length δ, assumed to be at a spatially independent temperature. The enthalpy balance over this inert zone yields the following modified boundary conditions

$$\xi = \xi_{in} \qquad \mathrm{Le}\,\delta \frac{\partial y}{\partial \tau} - \frac{1}{\mathrm{Pe}_y}\frac{\partial y}{\partial \xi} = \nu(y - y^{in}) \tag{6}$$

Note that at steady state or with $\delta \to 0$ this condition is reduced to the Danckwerts' condition (Eq. 4). This condition is used in one case below.

A general continuous model (infinite port model)

To facilitate the analysis of the emerging patterns and the parameter space we consider the limiting case of an infinite-port loop reactor ($N \to \infty$). In this case the stepwise functions $\xi_{in}(\tau)$, $\xi_{out}(\tau)$ can be replaced by continuously varied functions

$$\zeta_{in}(\tau) = \xi_{in}^0 - V_{sw}\tau \qquad \zeta_{out}(\tau) = \xi_{out}^0 - V_{sw}\tau$$

where the *switching velocity* (V_{sw}) is defined as $V_{sw} = \Delta L/\sigma$. In such a case it is convenient to transform the governing Eqs. 3 using a moving coordinate system ($\tau' = \tau$, $\zeta = \xi - V_{sw}\tau$) with fixed positions of the inlet and outlet:

$$\mathrm{Le}\frac{\partial y}{\partial \tau} + (\nu - \mathrm{Le}\,V_{sw})\frac{\partial y}{\partial \zeta} - \frac{1}{\mathrm{Pe}_y}\frac{\partial^2 y}{\partial \zeta^2} = B\,\mathrm{Da}(1-x)\exp\left(\frac{\gamma y}{\gamma + y}\right)$$
$$\frac{\partial x}{\partial \tau} + (\nu - V_{sw})\frac{\partial x}{\partial \zeta} - \frac{1}{\mathrm{Pe}_x}\frac{\partial^2 x}{\partial \zeta^2} = \mathrm{Da}(1-x)\exp\left(\frac{\gamma y}{\gamma + y}\right) \tag{7}$$

In the noncompact scheme traditional Danckwerts' boundary conditions can be applied (with ξ replaced by ζ). For a compact organization preliminary simulations have shown that this condition does not allow us to predict the temperature decline downstream from the reaction zone, which is observed in the discrete model simulations with finite N. To take this effect into account it is reasonable to consider the possible interaction of the inlet and outlet ports by conduction. We can also assume that there is a narrow inert domain between the feed and exit ports. This will require a special organization in the space between these ports, which will probably make it technically difficult. Alternatively, if conduction through the reactor wall is significant, it will achieve the same effect. In the limit of such

a very narrow, inert section the matched boundary conditions can be derived as a continuity of the temperature and a steady-state enthalpy balance that incorporates the contribution of the inlet and outlet fluxes from the neighboring sections

$$y|_{in} = y|_{out} \qquad \frac{1}{\mathrm{Pe}_y}\left(\left.\frac{\partial y}{\partial \zeta}\right|_{in} - \left.\frac{\partial y}{\partial \zeta}\right|_{out}\right) = \nu(y - y^{in}) \qquad (8)$$

Equation system 7, with the appropriate boundary conditions, corresponds to the limiting case of the discrete port system with $N \to \infty$ for any switching velocity. For a case of a fast-switching velocity it is possible to derive (see below) an asymptotic continuous model that can be used as a guide in the case $V_{sw} \to \infty$, $N \to \infty$.

Fast-switching asymptote

Let the switching velocity V_{sw} (that is, $L/N\sigma$) be significantly faster than the pattern motion, and moreover the switching cycle ($\theta = N\sigma$) is significantly smaller than all characteristic timescales (including conduction, diffusion, and chemical reaction). Then we can define the switching cycle–averaged variables $\bar{y}(\tau, \xi)$, $\bar{x}(\tau, \xi)$. In the limit of many ports and fast switching the $\bar{y}$ and $\bar{x}$ profiles are continuous and the supply can be integrated into the balance equations as if the feed is evenly distributed (see Appendix)

$$\mathrm{Le}\frac{\partial \bar{y}}{\partial \tau} + \nu\frac{\partial \bar{y}}{\partial \xi} - \frac{1}{\mathrm{Pe}_y}\frac{\partial^2 \bar{y}}{\partial \xi^2} = B\,\mathrm{Da}(1-\bar{x})\exp\left(\frac{\gamma\bar{y}}{\gamma+\bar{y}}\right) - \frac{\nu}{L}(\bar{y} - y^{in}) = f(\bar{y}, \bar{x})$$

$$\frac{\partial \bar{x}}{\partial \tau} + \nu\frac{\partial \bar{x}}{\partial \xi} - \frac{1}{\mathrm{Pe}_x}\frac{\partial^2 \bar{x}}{\partial \xi^2} = \mathrm{Da}(1-\bar{x})\exp\left(\frac{\gamma\bar{y}}{\gamma+\bar{y}}\right) - \frac{\nu}{L}(\bar{x} - x^{in}) = g(\bar{y}, \bar{x}) \qquad (9)$$

Slow Switching

In the first part of this section we consider the pattern-formation mechanism predicted by the limiting model (Eq. 7) and determine the domain of slow-switching patterns. In the second part we present and compare numerical simulations of both continuous and discrete section models (Eq. 3). We want to verify that the discrete model with N units converges the limiting one with $N \to \infty$.

Analytical results

Inspection of the problem statement (Eqs. 7 with the appropriate boundary conditions) shows that this system is quite similar to that of a front propagation in a fixed bed with the switching velocity V_{sw} replaced by the front velocity V_{fr}. The main difference between these two problems is the boundary conditions applied (in the front propagation problem an infinitely long system is traditionally considered with the no-flux BC behind the front). If the length L is sufficiently large, we expect to find in the loop reactor with $V_{sw} = V_{fr}$ frozen solutions in the form of a front or a pulse that rotates in the physical coordinate system. Moreover, we expect that such a "frozen" rotating pattern can be sustained for a domain of V_{sw} that lies between the combustion front velocity V_{fr} and the velocity of the thermal front $V_{th} = 1/\mathrm{Le}$; (the condition $V_{fr} < 1/Le$ is explained below) that is

$$V_{fr} < V_{sw} < V_{th} \qquad (10)$$

This expectation and the effect of the applied boundary conditions (which differ from the classical problem of the front propagation in an unbounded domain) are verified by numerical simulations below. The velocity of the front propagation and its stability have been intensively studied since publication of the classical works of Frank-Kamenetski[18] and Zeldovich and Barenblatt[19] half a century ago. To a first approximation we use the approximate relations for V_{fr} and the related property: the maximum increase of temperature on the front ΔT_m, recently proposed by Burghardt et al.[20] This derivation is based on the concept of the ideal thermal front (by Frank-Kamenetski[18]) with negligible mass diffusion ($\mathrm{Pe}_x \to \infty$), coupled with the extrapolation technique of the temperature profile from the low-T zone to the reaction zone,[21] and yields a set of algebraic equations that can be applied in a domain $\mathrm{Le} > 1$, $V_{fr} < \mathrm{Le}^{-1}$

$$\vartheta_a\vartheta_m^2\left(\frac{\mathrm{Le}-1}{\vartheta_m\mathrm{Le} - \vartheta_a}\right)^2 = \frac{\mathrm{Da}_0}{\gamma\,\mathrm{Pe}_L}(1+\vartheta_m)^2\exp\left(\frac{-\gamma}{\vartheta_m+1}\right)$$

$$V_{fr} = \frac{1 - \vartheta_a/\vartheta_m}{\mathrm{Le} - \vartheta_a/\vartheta_m} \qquad (11)$$

Here $\vartheta_m = \Delta T_m/T_0$, $\vartheta_a = \Delta T_a/T_0$ (the dimensionless adiabatic temperature increase), $\mathrm{Da}_0 = \tilde{L}A/u$, and $\mathrm{Pe}_L = \mathrm{Pe}_y Lv$ (that is, the Damkohler and Peclet numbers, respectively, are defined by the reactor length and the convective velocity).

Because $\mathrm{Le} \gg 1$ in catalytic reactors, the domain of "frozen" rotating patterns corresponds to low switching velocities ($V_{sw} < \mathrm{Le}^{-1} \ll 1$) with respect to the convective velocity. Note that these patterned states can coexist with pseudo-homogeneous extinguished solutions and their selection depends on the choice of the initial conditions.

Numerical simulations

Numerical simulations presented below were conducted for the compact organization scheme. We used two sets of parameters borrowed from a study of a flow-reversal reactor by Eigenberger and Nieken,[3] which differ in feed parameters (T^{in} and C^{in}; see Table 1) and the corresponding behavior of the steady-state solutions of the asymptotic model (Eq. 9). In both cases there exists a single (extinguished) steady state, which is stable in case 1 and admits a bifurcation to moving waves (see below) in case 2. In Table 1, which lists the parameters used in simulations, we also outlined the adiabatic temperature increase (ΔT_a), the analytically predicted values of the front velocity and the maximal temperature (V_{fr}^a, T_m^a, Eqs. 11), and the corresponding numerical values (V_{fr}^n, T_m^n), which were obtained in preliminary simulations of a long one-section model. For both sets the analytically and numerically calculated parameters are in a good agreement.

Discrete Model (Eq. 3). A typical rotating-pattern solution

Table 1. Two Sets of the Inlet and the Corresponding Critical Characteristics*

Parameter	Set 1	Set 2
$C^{in} \times 10^4$, kmol/m^3	1.21	4.6
T^{in}, C	293	409
ΔT_{ad}, C	50	194
$V^a_{fr} \times 10^3$, m/s	1.185	0.954
$V^n_{fr} \times 10^3$, m/s	1.18	0.92
T^a_m, C	977	1207
T^n_m, C	957	1088
T_s, C	293	505
$C_s \times 10^4$, kmol/m^3	1.21	2.28
$V^a_r \times 10^3$, m/s	—	1.161
$V^n_r \times 10^3$, m/s	—	1.167

*Other parameters (after Eigenberger and Nieken[3]): $(-\Delta H) = 206{,}000$ kJ/mol; $\rho C_{pe} = 400$ kJ m^{-3} K^{-1}; $\rho C_{pf} = 0.5$ kJ m^{-3} K^{-1}; $k = 0.002$ kW/mK; $D_f = 0.005$ m^2/s; $A = 29{,}732$ l/s; $E/R = 8000$ K; $L = 1$ m; $u = 1$ m/s (corresponding Le = 800, Pe$_y$ = 194, Pe$_x$ = 200).

of a four-unit system with a certain switching velocity V_{sw} in a domain $V_{fr} < V_{sw} < V_{th}$ is shown in Figure 2 (parameters of set 1). The pattern is evident from the gray-scale presentation of the temperature field (Figure 2a1); certain changes in T occur within the cycle, and the changes are significantly more pronounced in the conversion stairway-like gray-scale plot (Figure 2b1). The spatial temperature profile (Figure 2a2; Figure 4) is relatively smooth and exhibits a high temperature, much higher than the adiabatic temperature increase (50°C). At any given position the temperature oscillates in time (Figure 2a3), as the pattern propagates along the loop, and typically exhibits much lower values in the section adjusted to the flow-exit point

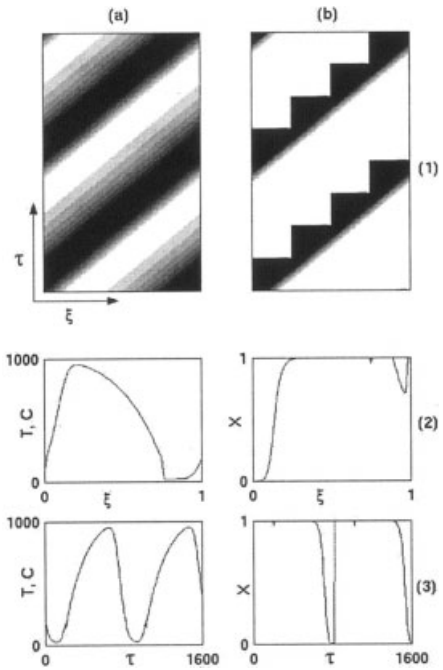

Figure 2. Typical moving wave solution of a four-unit loop reactor in the case of slow switching.

Row 1 shows spatiotemporal gray-scale patterns of the dimensionless temperature (a) and concentration (b); row 2 presents typical snapshots of spatial profiles; row 3 shows temporal profiles at a certain cross section. Parameters of set 1 with $V_{sw} = 0.00122$ m/s.

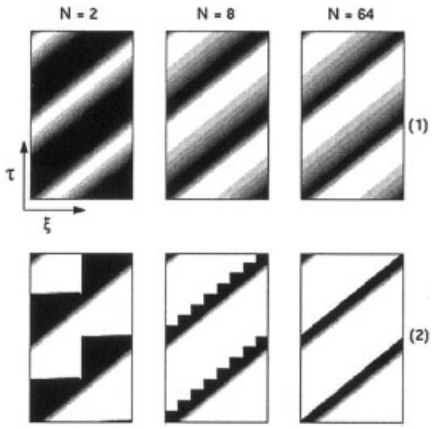

Figure 3. Effect of number of units (*N*) on the spatiotemporal patterns of the temperature (upper row) and concentration (lower row).

Parameters as in Figure 2.

(which is switched in a stepwise way) than those within the reactor. At the same time both spatial (Figure 2b2) and temporal profiles of the concentration (Figure 2b3) are sharp and exhibit practically full conversion for most of the reactor, excluding the first section that adjusts itself to the inlet.

With increasing number of ports (N), while preserving the same switching velocity V_{sw}, the stairlike patterns become smoother (Figure 3). The temperature (Figure 4a) and concentration profiles with $N \to \infty$ converge to certain limiting solutions. This aspect is also illustrated by the plot of maximal temperature T_m vs. inverse number of units (Figure 4b).

The obtained results obviously corroborate the existence of the *limiting continuous model* (Eqs. 7). To implement this model we need first of all to verify the effect of applied boundary conditions and to choose the most suitable one (see discussion above). We tested three different sets of BC: (1) the traditional Danckwerts' BC (Eq. 4), (2) matched BC defined by equation set 8, and (3) fixed temperature and concentration on

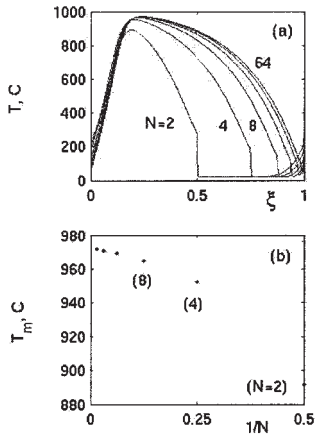

Figure 4. Effect of number of units (*N*) on the spatial temperature profiles (a) and the maximal temperature (b) showing convergence with increasing *N* to a limiting solution.

Numbers denote N; other parameters as in Figure 2.

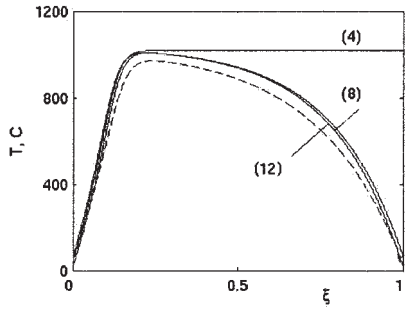

Figure 5. Effect of the boundary conditions on the temperature profiles calculated by continuous limiting model (Eqs. 7).

Numbers in parentheses mark the equation of the corresponding boundary condition (BC). Dashed line denotes the 64-unit solution. Parameters as in Figure 2.

both boundaries; the latter may be considered as the limiting case of the matched BC with Pe_y, $Pe_x \rightarrow \infty$ along with an assumption of a complete conversion:

$$y(0) = y(L) = y^{in} \qquad x(0) = x^{in} \qquad x(L) = 1 \qquad (12)$$

As expected the Danckwerts' BC cannot predict the temperature decline in the downstream region (Figure 5). The profiles calculated with the other BC (Eqs. 8 and 12) are in good agreement with numerical simulations of a reactor with many ports ($N > 64$; Figure 5). Boundary conditions affect the profiles to some degree: the minimal temperature is better predicted in the case of small N (and large Pe) by conditions in Eq. 12, whereas in the case of large N equation set 8 is preferential; the maximal temperature practically does not depend on the BC. Summarizing these results we chose BC (Eq. 8) for the following simulations since it seems physically more reasonable and less restrictive.

Now we can study the parameter domain and the pattern characteristics using the limiting continuous model and the validated BC. Changing V_{sw} strongly affects the solution (Figure 6): traveling waves exist in a narrow domain of parameters approximately following condition 10 with 1.175 m/s $< 10^3 \times V_{sw} <$ 1.285 m/s in our case; outside this domain only the extinguished solution exists. The limiting model predicts well the results of a discrete section reactor: in the four-unit system the patterns exist in a slightly narrower domain (1.19 m/s $< 10^3 \times V_{sw} <$ 1.27 m/s) and the maximal temperature differs from the limiting values by not more than 7% (Figure 7). Note that the discrepancy between the discrete and continuous model decreases with increasing N (see also Figure 4b). Figure 7 also shows good agreement between the analytically and numerically obtained front velocities (V^a_{fr}, V^n_{fr}) and the corresponding maximal temperatures (T^a_m, T^n_m), and completely confirms condition 10, which defines the domain of the slow-switching patterns.

The effect of varying heat- and mass Peclet numbers (Pe_y, Pe_x) is shown in Figure 8. The effect of increasing Pe_x is negligible, whereas increasing Pe_y leads to higher maximal temperatures and the solution approaches the behavior of a square wave. The domain of the switching velocities for which the pattern state exists is predicted by condition 10 as well.

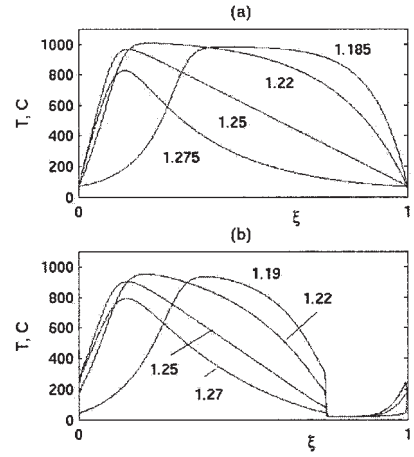

Figure 6. Effect of the switching velocity V_{sw} on the spatial temperature profiles simulated with the limiting model (Eqs. 7 and 8) (a) and a four-unit model (b).

Numbers denote $V_{sw} \times 10^3$ m/s. Other parameters as in Figure 2.

Similar results were obtained with parameters of set 2.

Fast Switching

In the first part of this section we consider the pattern-formation mechanism predicted by the limiting model (Eq. 9). In the second part we present the results of numerical simulations using both the continuous models (Eqs. 7 and 9) and the discrete section model (Eqs. 3, 4). We focus attention on the effects of the switching velocity V_{sw} and of the number of units N.

Analytical results

The unique feature of the limiting model (Eq. 9) is that, aside from the boundaries, the system can attain an asymptotic spatially homogeneous solution (y_s, x_s) defined by the zeros of

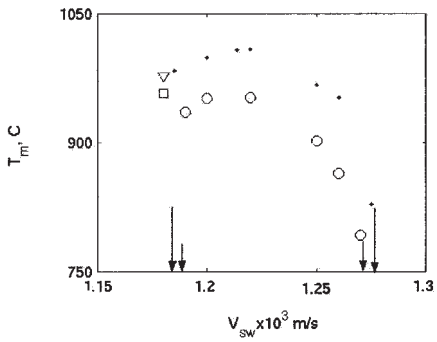

Figure 7. Bifurcation diagrams showing the effect of the switching velocity V_{sw} on the maximal temperature T_m in a four-unit system (○) and in the limiting model (Eq. 7, dots).

The analytically (Eqs. 11) and numerically calculated sets (front velocity, maximal temperature) are marked by ▽ and □, respectively. The short and long arrows mark the extinction limits in a four-unit system and in a limiting model, respectively. Parameters of set 1.

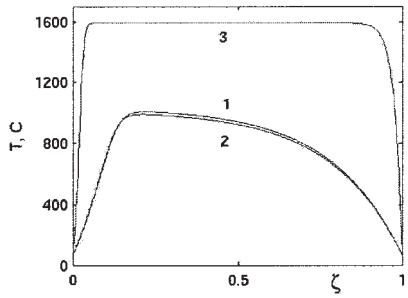

Figure 8. Effect of varying of the heat- (Pe_y) and mass-Peclet (Pe_x) numbers showing the simulated temperature profiles.

Curve 1: $Pe_y = 194$, $Pe_x = 200$; curve 2: $Pe_y = 194$, $Pe_x = 2000$; curve 3: $Pe_y = 1940$, $Pe_x = 200$. Other parameters as in Figure 2.

the right-hand sides: $f(y_s, x_s) = g(y_s, x_s) = 0$ and up to three solutions may exist within a certain set of parameters. The steady-state solutions (SS) or steady rotating patterns of Eqs. 9, with Pe_y, $Pe_x \to \infty$, are described essentially by a mixed-reactor model (CSTR) with spatial behavior replacing the temporal one. We should thus expect that model 9 with finite Pe_y, Pe_x may exhibit a rich plethora of patterned states that bifurcate from a homogeneous SS as we change a parameter (such as Pe_y, Pe_x) and can be classified according to an asymptotic behavior of the corresponding CSTR model.[16,17]

To find an inhomogeneous solution of equation set 9 in the form of a single-period wave rotating over the loop with a certain velocity V_r, we conducted a linear stability analysis. Note that, contrary to the approach applied for the general continuous model (Eqs. 7), this velocity is not related with the switching velocity V_{sw}, which is assumed to be infinitely large, but rather with the intrinsic properties of the system. Denoting the deviation from the basic steady state solution $\mathbf{U} = \{x_s, y_s\}$ as $\mathbf{u} = \{\hat{x}, \hat{y}\}$ and linearizing the original problem, we arrive at the following system for the perturbations

$$\begin{aligned} \mathrm{Le}\frac{\partial \hat{y}}{\partial \tau} + \nu\frac{\partial \hat{y}}{\partial \xi} - \frac{1}{\mathrm{Pe}_y}\frac{\partial^2 \hat{y}}{\partial \xi^2} &= j_{11}\hat{y} + j_{12}\hat{x} \\ \frac{\partial \hat{x}}{\partial \tau} + \nu\frac{\partial \hat{x}}{\partial \xi} - \frac{1}{\mathrm{Pe}_x}\frac{\partial^2 \hat{x}}{\partial \xi^2} &= j_{21}\hat{y} + j_{22}\hat{x} \end{aligned} \qquad (13)$$

where j_{km} represents the components of the Jacobian matrix $d[f, g]/d[\bar{y}, \bar{x}]$ estimated at the steady state. Looking for a "frozen" solution rotating with a velocity V_r, we can reduce the system of equations 13 to a set of ordinary differential equations with $\eta = \xi - V_r\tau$

$$\begin{aligned} (\nu - \mathrm{Le}\,V_r)\hat{y}_\eta - \mathrm{Pe}_y^{-1}\hat{y}_{\eta\eta} &= j_{11}\hat{y} + j_{12}\hat{x} \\ (\nu - V_r)\hat{x}_\eta - \mathrm{Pe}_x^{-1}\hat{x}_{\eta\eta} &= j_{21}\hat{y} + j_{22}\hat{x} \end{aligned} \qquad (14)$$

Assuming the perturbations to be harmonic in the space variable η, that is, $\mathbf{u} \sim e^{ik\eta}$, where k is the perturbation wave number, and by substituting this expression into Eqs. 14 we obtain a homogeneous system with respect to the perturbation amplitudes with a determinant D

$$D = \begin{vmatrix} ikq + \dfrac{k^2}{\mathrm{Pe}_y} - j_{11} & -j_{12} \\ -j_{21} & iks + \dfrac{k^2}{\mathrm{Pe}_x} - j_{22} \end{vmatrix} \qquad (15)$$

where $q = \nu - \mathrm{Le}\,V_r$ and $s = \nu - V_r$. The bifurcation condition ($D = \mathrm{Re}\,D + i\,\mathrm{Im}\,D = 0$) is reduced to the following set of relations

$$\begin{aligned} \mathrm{Re}\,D &= k^4\frac{1}{\mathrm{Pe}_y\mathrm{Pe}_x} - k^2\left(qs + \frac{j_{22}}{\mathrm{Pe}_y} + \frac{j_{11}}{\mathrm{Pe}_x}\right) - \Delta = 0 \\ \mathrm{Im}\,D &= k^2\left(\frac{s}{\mathrm{Pe}_y} + \frac{q}{\mathrm{Pe}_x}\right) - sj_{11} - qj_{22} = 0 \end{aligned} \qquad (16)$$

where $\Delta = j_{11}j_{22} - j_{21}j_{12}$. Given that the target wave number k is known ($k = 2\pi/L$), equation set 16 allows us to determine the value of the prescribed bifurcation parameter and the rotation velocity V_r. Note that in the limiting case $\mathrm{Pe}_y \to \infty$, which is of practical interest, the equations above can be significantly simplified and reduced to

$$-k^2\left(qs + \frac{j_{22}}{\mathrm{Pe}_y}\right) - \Delta = 0 \qquad k^2\frac{s}{\mathrm{Pe}_y} - sj_{11} - qj_{22} = 0 \qquad (17)$$

The approach described above can be applied directly to determine V_r if the emanating branch of oscillatory solutions is stable. This is essentially a Hopf bifurcation to spatial periodic rotating patterns. Using continuation methods (the software package AUTO[22]) we traced the bifurcation diagrams with V_r as a bifurcation parameter (Figure 9, set 2). The oscillatory branch originating from a Hopf point (Eq. 16, with $k = 2\pi$ and $V_r = 0.00121$ m/s), which is subcritical in this case (H_1, Figure 9), passes two limit points of periodic patterns ($LP_{1,2}$, Figure 9b) and terminates at a second Hopf point with smaller $V_r = 0.00117$ m/s and $k = 2.8$ (H_2, Figure 9). Thus, the wave number (k) or the period of oscillations (P) exhibits nonmonotonic behavior with V_r, which allows determination of a stable solution that exactly matches the system size $L = P = 1.0$ m at a certain V_r^a (0.001161 m/s, Figure 9c).

Note that the bifurcation diagram may be significantly more complicated, depending on the governing parameters, and for a comprehensive study we need to consider other possible situations. This was demonstrated in several similar studies devoted to patterns in a cross-flow reactor,[16,23] which is quite similar to the loop reactor except for the periodic boundary conditions. However, such a problem is beyond the scope of the present paper. Recall also that the oscillatory and other possible complex solutions of equation system 9 correspond to the limiting solutions of Eqs. 3 with $V_{sw} \to \infty$, $N \to \infty$. This information can be used as a *guide* for the following analysis. For finite V_{sw}, N we expect to find complex solutions with superposition of two main frequencies: $\omega_{sw} = 2\pi V_{sw}/L$ and $\omega_r = 2\pi V_r^a/L$.

Numerical simulations

Rotating patterns are demonstrated (with set 2 using higher feed conditions T^{in}, C^{in}) using either the limiting continuous

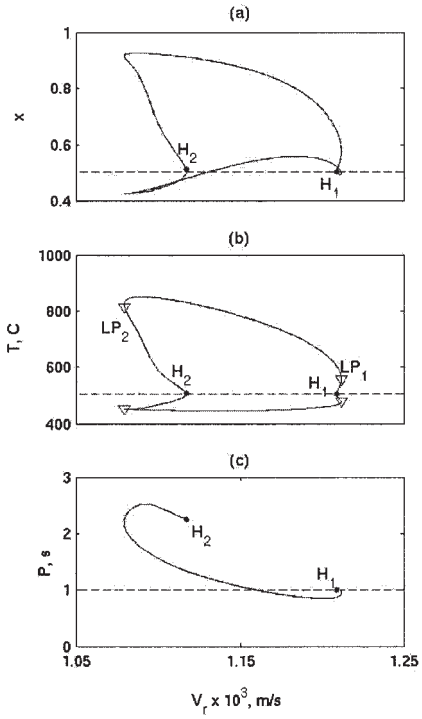

Figure 9. Bifurcation diagrams of oscillatory behavior of conversion *x* (a) temperature *T* (b), and the period of oscillation *P* (c) with varying rotation velocity V_r.

Dots: the Hopf bifurcations (H_1, H_2); ▽: the limit points (LP_1, LP_2). Dashed lines mark the steady state solution.

models (Eqs. 7 or Eqs. 9) or the discrete unit model (Eq. 3) with the Danckwerts' BC.

The analytical predictions were confirmed by numerical simulations of the *asymptotic model* (Eq. 9): the sustained pattern is a simple wave (Figure 10a), rotating around the loop at velocity $V_r^n = 0.001167$ m/s, which is in excellent agreement with the corresponding analytical value ($V_r^a = 0.001161$ m/s). Simulations of the *discrete model* (Eq. 3) with large V_{sw} revealed a complex pattern with two different lengths and timescales (Figure 10b): the large amplitude waves, having a wavelength equal to the reactor length L, propagate at velocity V_l ($\approx$0.011 m/s) are superimposed with small-amplitude oscillations with a wavelength of L/N that propagate with the switching velocity (V_{sw}).

The number of units strongly affects the sustained patterns. With small N (=2, Figure 10b) the rotating patterns exhibit an oscillatory behavior: the ignited pulse expands and propagates downstream with increasing temperature along each section. Port switching leads to the abrupt decline in local temperature and dramatic transformation of the temperature profile along the whole reactor (Figure 10b3). With increasing N the large-amplitude waves become more homogeneous (the impact of the small-amplitude modulation becomes increasingly less pronounced) and with $N \geq 8$ the rotating waves become practically "frozen." The maximal temperature and maximal conversion slightly decrease with increasing N, and all the spatial profiles tend to the limiting solution predicted by the model in Eqs. 9. The period of large-amplitude oscillations varies slightly with N and tends to the limiting value with $N \to \infty$ as well.

With increasing switching velocity V_{sw} the discrete model results converge to the limiting solution.

For conditions that do not produce rotating patterns [that is, when system 9 does not satisfy the bifurcation condition (Eq. 16)] we expect to find a quasi-steady (nonrotating) solution or multiple such solutions. This is demonstrated with set 1, which shows a pseudo-homogeneous solution of a high temperature and practically full conversion (Figure 11). This simulation used modified BCs that account for a narrow inert entrance zone (Eq. 9). Local changes in the narrow regions, adjusted to the inlet of each section, practically do not affect the rest of the reactor, and even more so, the outlet parameters. With increasing number of units the maximal temperature decreases and the solution tends to the extinguished state predicted by the limiting model.

Simulations of the discrete-port model (Eq. 3) with N = 2–32 and the Danckwerts' BC yield only the extinguished states for all V_{sw} values used. As argued above the extinguished solutions may be attributable to the pseudo-homogeneous model used in our work and future work will test a heterogeneous model with more natural BCs.

Intermediate Switching

A rich plethora of patterns, depending both on the switching velocity V_{sw} and number of units N, was obtained with V_{sw}/V_{fr}

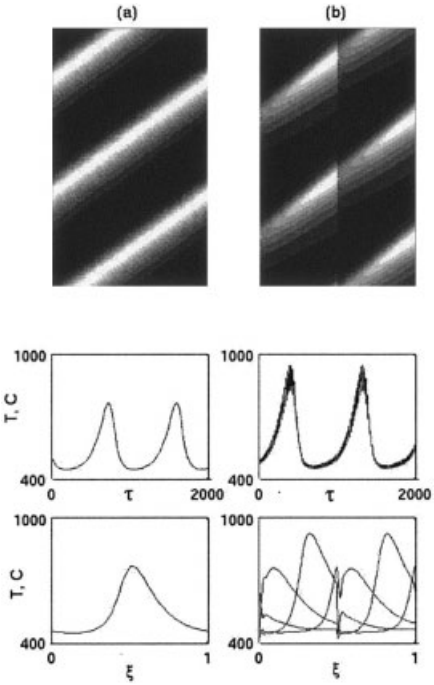

Figure 10. Rotating pulse solution of (a) the asymptotic model (Eqs. 9) and (b) a two-unit loop reactor (Eqs. 3) (V_{sw} = 0.5 m/s).

Row 1 presents the spatiotemporal gray-scale patterns of the dimensionless temperature. Row 2 shows the temporal profiles at a certain cross section ($\xi = 1$ for a discrete model). Row 3 shows the limiting spatial profile (a) and several snapshots of equal time intervals for $N = 2$ model (b). Parameters of set 2.

that varies between the two asymptotes. It is beyond the scope of this work to unravel the structure of solutions in this domain and we present only few cases.

Several typical patterns simulated with a *discrete* two-unit model (Eqs. 3) and intermediate switching velocities (Figures 12b and c) exhibit multiple oscillating pulses traveling over the loop (compared with a single continuous rotating pulse in the slow-switching case; Figure 12a). Both low-temperature patterns with incomplete conversion (V_{sw} = 0.0025 m/s; Figure 12b) and high-temperature structures (V_{sw} = 0.0081 m/s; Figure 12c) emerge. These patterns can be regular with simple oscillations, multiperiodic, or even complex (irregular). Within certain domains of V_{sw}/V_{fr} the system admits complex solutions with a global period that includes several (say n) large-amplitude oscillations superimposed with a certain number of small-amplitude oscillations (say m). Let us denote such solutions as $L_n s_m$ structures (such as the $L_2 s_{15}$ pattern in Figure 12c). With increasing V_{sw} the impact of the small-amplitude oscillations becomes increasingly less pronounced and such complex patterns are transformed into $L_1 s_m$ structures, typical for the fast-switching regimes.

Concluding Remarks

Although the loop reactors have been numerically investigated in the past 5 years, using kinetic models that correspond to VOC combustion[10,11] or various reversible gas synthesis reactions,[12-14] the present work is the first systematic study of the behavior asymptotes of such reactors. This study explains some of results produced by Barresi and coworkers, including the high temperatures at slow switching and low temperatures at fast switching. This study reveals other novel possible features such as multiplicity of solutions, rotating pulses with high temperatures at fast switching, and a complex structure of low- and high-temperature windows as the ratio of switching to front velocity is varied.

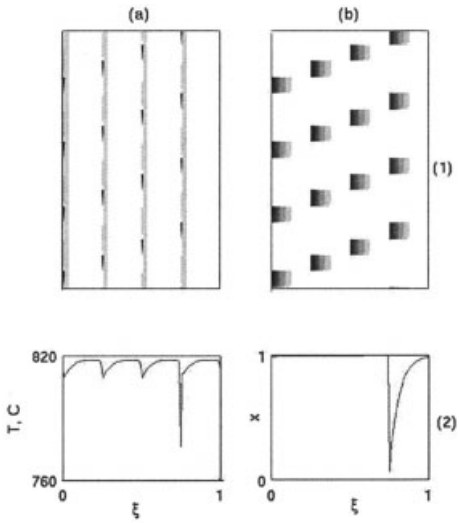

Figure 11. A pseudo-homogeneous solution of a four-unit reactor in the case of fast switching.

Row 1 shows spatiotemporal gray-scale patterns of the temperature (a) and concentration (b). Row 2 presents spatial profiles at a certain time moment. Parameters of set 1, V_{sw} = 0.25 m/s (only is this case the BC of Eq. 6 was applied).

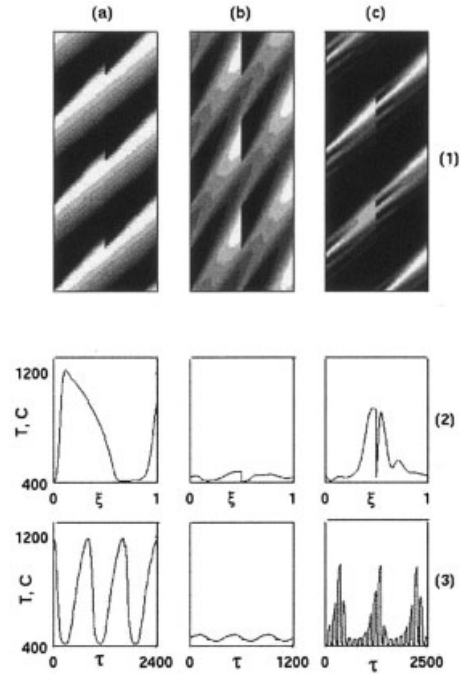

Figure 12. Effect of switching velocity V_{sw} on emerging patterns in the case of intermediate switching.

Row 1 shows spatiotemporal gray-scale patterns of the dimensionless temperature. Row 2 presents typical snapshots of spatial profiles. Row 3 shows temporal profiles at a certain cross section (ξ = 1). V_{sw} = 0.00122 m/s [(a), a slow-switching regime], 0.0025 m/s [(b), a low-temperature regular pattern], and 0.0081 m/s [(c), a high-temperature multiperiodic pattern with $L_2 s_{15}$ structure]. N = 2, parameters of set 2.

Two limiting models of the loop reactor are derived: The first one corresponds to the case of an infinite number of units and arbitrary switching velocities, whereas the second model describes the asymptotic case of an infinite number of ports with large switching velocities and is essentially a cross-flow model.

Rotating pulses can be obtained by either slow or fast switching. The former case can be sustained when the switching velocity is nearly similar to the front velocity of the same system in a long reactor. When that ratio exceeds a certain domain around unity the rotating pulse collapses. The limiting model allows us to determine the domain of parameters that sustain the rotating pulse and to predict the pulse properties (maximal temperature increase). These conclusions are confirmed by direct numerical simulation showing good agreement between the limiting continuous model and the realistic discrete model with $N > 4$. In summarizing the slow-switching results we can conclude that the reactor design and operation are highly sensitive to design parameters, and control of switching time should be advantageous. However, high temperatures can be attained over a wide domain of parameters. Peak temperatures probably somewhat exceed the hot spot attained in flow-reversal reactors, and as in the latter the temperature increases as the feed flow rate is increased. Be-

cause this reactor exhibits a domain of declining temperatures (and ascending conversions) even in adiabatic units, it should be tested with exothermic reversible reactions, and may be superior to flow-reversal reactors for that purpose.

In the case of *fast switching* a rich plethora of patterns may be sustained, although this requires that parameters lie within a certain domain around the boundary where the limiting model admits a spatial Hopf bifurcation. As demonstrated this can be achieved in a reactor of reasonable length. Because it is an asymptotic solution, then such a solution can be sustained over a wide domain of switching velocities and will not require special control. Varying the ratio of switching to front velocity will reveal a complex structure of alternated windows of "hot" and "cold" states. For a small number of units the system exhibits complex patterns that are formed by interaction of the large-amplitude rotating wave (close to the analytical solution), modulated by small-amplitude oscillations. This feature will be the subject of further studies.

The fast-switching asymptote can produce rich dynamics and complex bifurcation diagrams: These features were studied for the same kinetics in a cross-flow reactor,[16,17,23] which is quite similar to the loop reactor except for the boundary conditions. The former was shown to exhibit almost homogeneous ignited states, multiplicity of stationary patterns, and, in the case of two reactions, stationary spatially complex patterns. We expect to find similar features for loop reactors.

This study is a first step in construction of the limiting models of the loop reactor. Natural extensions of this research will include:

(1) A heterogeneous model that accounts for heat- and mass-transfer resistances between phases; in that case the effect of flow velocity on the front velocity will be weaker and, consequently, the domain of existence of pulse solutions in the fast-switching mode will be wider.

(2) Applications to reversible exothermic reactions will require matching of the declining temperature profile of the pulse to the optimal solution that relates conversion and temperature.

(3) Applications to the coupling of endothermic and exothermic reactions (such as methane reforming and oxidation), with several feed points at any time. We can now imagine an asymptotic solution with two moving feed ports, in which the reactants of either reaction are fed, as well as two moving exit ports. Other strategies of port placing can be suggested as well.

Acknowledgments

M. Sheintuch is a member of the Minerva Center of Nonlinear Dynamics. O. Nekhamkina is partially supported by the Center for Absorption in Science, Ministry of Immigrant Absorption State of Israel.

Literature Cited

1. Matros YuSh, Bunimovich GA, Noskov AS. The decontamination of gases by unsteady-state catalytic method: Theory and practice. *Catalysis Today*. 1993;17:261-273.
2. Noskov AS, Bobrova LN, Matros YuSh. Reverse-process for NOx—Off gases decontamination. *Catalysis Today*. 1993;17:293-300.
3. Eigenberger G, Nieken U. Catalytic combustion with periodic flow reversal. *Chemical Engineering Science*. 1988;43:2109-2115.
4. Kolios G, Frauhammer J, Eigenberger G. Autothermal fixed-bed reactors concepts. *Chemical Engineering Science*. 55, 5495 (2000).
5. Boreskov GK, Matros YuSh, Kiselev OV. Catalytic processes under nonsteady-state conditions. I. Thermal front in the immobile catalyst layer. *Kinetics and Catalysis.* 20:773-780 (1979).
6. Boreskov GK, Matros YuSh. Unsteady state performance of heterogeneous catalytic reactions. *Catalysis Reviews—Science and Engineering*. 1983;25:551-590.
7. Matros YuSh. *Catalytic Processes Under Unsteady-State Conditions*. Amsterdam: Elsevier; 1989.
8. Gerasev AP, Matros YuSh. Nonsteady-state process for ammonia synthesis. *Teoreticheskie Osnovy Khimicheskoi Tekhnologii*. 1991;25:821-827.
9. Vanden Bussche KM, Froment GF. The STAR configuration for methanol synthesis in reversed flow reactors. *Canadian Journal of Chemical Engineering*. 1996;74:729-734.
10. Brinkmann M, Barresi AA, Vanni M, Baldi G. Unsteady state treatment of very lean waste gases in a network of catalytic burners. *Catalysis Today.* 1999;47:263-277.
11. Fissore D, Barresi AA. Comparison between the reverse-flow reactor and a network of reactors for the oxidation of lean VOC mixtures. *Chemical Engineering and Technology*. 2002;25:421-426.
12. Fissore D, Barresi AA, Baldi G. Synthesis gas production in a forced unsteady-state reactor network. *Industrial and Engineering Chemistry Research*. 2003;42:2489-2495.
13. Velardi SA, Barresi AA. Methanol synthesis in a forced unsteady-state reactor network. *Chemical Engineering Science*. 2002;57:2995-3004.
14. Velardi S, Barresi AA, Manca D, Fissore D. Complex dynamic behavior of methanol synthesis in the ring reactor network. *Chemical Engineering Journal*. 2004;99:117-123.
15. Yakhnin VZ, Rovinsky AB, Menzinger M. Differential flow instability of the exothermic standard reaction in a tubular cross-flow reactor. *Chemical Engineering Science*. 1994;49:3257-3262.
16. Nekhamkina OA, Nepomnyashchy AA, Rubinstein BY, Sheintuch M. Nonlinear analysis of stationary patterns in convection-reaction-diffusion systems. *Physical Review E*. 2000;61:2436-2444.
17. Nekhamkina OA, Rubinstein BY, Sheintuch M. Spatiotemporal patterns in thermokinetic model of cross-flow reactors. *AIChE Journal.* 2000;46:1632-1640.
18. Frank-Kamenetski DA. *Diffusion and Heat Exchange in Chemical Kinetics*. New York, NY: Princeton University Press; 1955.
19. Zeldovich YuB, Barenblatt GI. Theory of flame propagation. *Combustion and Flame*. 1959;2:61-74.
20. Burghardt A, Berezowski M, Jacobsen EW. Approximate characteristics of a moving temperature front in a fixed-bed catalytic reactor. *Chemical Engineering and Processing*. 1999;38:19-34.
21. Kisielev OV. *Theoretical Study of the Phenomena of Heat Waves Movement in Catalytic Bed*. Novosibirsk, Russia: Russian Academy of Sciences, Institute of Catalysis; 1993 (in Russian).
22. Doedel EJ. AUTO, a program for the automatic bifurcation analysis of autonomous system. *Congressus Numerantium*. 1981;30:265-384.
23. Sheintuch M, Nekhamkina O. Stationary spatially-complex solutions in cross-flow reactors with two reactions. *AIChE Journal.* 2003;49:1241-1249.

Appendix

Derivation of the limiting model (Eq. 9)

Consider the enthalpy balance during one switching cycle for a control volume of the length $\Delta L = L/N$, which combines two halves of adjacent sections. The heat flux over each ith boundary (q_i, $i = 1, 2$) is continuous and accounts for convection and diffusion in a standard way: $\bar{q}_i = \nu\bar{y}\,|_i - \mathrm{Pe}_y^{-1}\bar{y}_\xi\,|_i$. The intermediate part of the control volume acts as the inlet/outlet during a short time interval σ and can be incorporated as additional internal sources $q_{in} = \nu y^{in}$, $q_{out} = \nu\bar{y}$ (the temperature does not vary during the short time interval σ). The resulting average value over the time interval θ is

$$\bar{q}_s = \nu\,\frac{\sigma}{\theta}\,(\bar{y} - y^{in}) = \nu\,\frac{\Delta L}{L}\,(\bar{y} - y^{in})$$

Now the total average balance over the control volume with the average chemical source term $\bar{q}_{chem}$ should be written as

$$\mathrm{Le}[\bar{y}(\tau+\theta,\xi)-\bar{y}(\tau,\xi)]\Delta L = \theta\left[(\bar{q}_2-\bar{q}_1)+\nu\frac{\Delta L}{L}(\bar{y}-y^{in})+\bar{q}_{chem}\Delta L\right]$$

By dividing the above equation by $\theta\Delta L$ we will obtain, in the limit $\theta,\ \Delta L \to 0$, a differential equation with respect to the average temperature:

$$\mathrm{Le}\frac{\partial\bar{y}}{\partial\tau}+\nu\frac{\partial\bar{y}}{\partial\xi}-\frac{1}{\mathrm{Pe}_y}\frac{\partial^2\bar{y}}{\partial\xi^2}=B\,\mathrm{Da}(1-\bar{x})\exp\left(\frac{\gamma\bar{y}}{\gamma+\bar{y}}\right)-\frac{\nu}{L}(\bar{y}-y^{in})$$

By conducting a similar procedure to the mass balance of the control volume we will obtain the fast-switching asymptote model (Eq. 9).

Manuscript received Jan. 13, 2004, and revision received May 10, 2004.